INTERNATIONAL JOURNAL OF SCIENTIFIC RESEARCH AND INNOVATIVE STUDIES
ISSN: 2820-7157
www.ijsrisjournal.com

**October 2024** **Volume 3** **Number 5** **Pages 06-16**

**Received Date:** August 19, 2024 **Accepted Date:** September 11, 2024 **Published Date:** October 14, 2024

Available Online at https://www.ijsrisjournal.com/index.php/ojsfiles/article/view/187

https://doi.org/10.5281/zenodo.13941446

# Kinetic Study of Nano Alumina on Absorption of Lead Ions in Aqueous Solution

**Almahdi R. Rabia[1, a], Masoud Mostafa Zatout[1, b]**

Faculty of Natural Resources and Environmental Science University of Derna, Libya

[a]A.Rabia@uod.edu.ly, [b]marwa.zatout@gmail.com

**Abstract:** The levels of lead (Pb) continue to rise in rivers and seawater. In many parts of the world, heavy metals such as lead in drinking water are found to have severe effects on human health. Thus, identifying effective and reliable methods for reducing these levels is crucial. This research explored the potential of using activated alumina as an adsorbent to reduce lead (Pb) ions from water. Powder activated alumina was produced from aluminum, with the precursor further processed into activated alumina. A design of experiments (DOE) using response surface methodology was employed to study the influence of pH, NaOH, HCl, DI (H2O), and Al (powder) on the quality and yield of activated alumina. The trend indicated that a higher amount of aluminum resulted in better adsorption performance. The micro-pore volume and cumulative pore volumes for the activated alumina were 0.000756 $cm^3/g$, 0.002050 $cm^3/g$, and 0.001976 $cm^3/g$, respectively. Kinetic studies were conducted to observe the reduction of heavy metal concentrations over time using activated alumina. The kinetics further confirmed that 95% of the lead was removed within the first 25 minutes of the experiment. The removal rate was rapid during the initial phase until equilibrium was reached at 25 minutes. Temperature, pH, and concentration were significant parameters, with lead ion removal increasing as the temperature rose to 60°C. The experimental results were in strong agreement with the Langmuir pseudo-second-order equation. This removal method using activated alumina is cost-effective, environmentally friendly, and holds significant potential for heavy metal removal from water. Therefore, this research demonstrated activated alumina as a promising adsorbent material for the removal of heavy metals from drinking water, contributing to the development of an economical product that can be applied to a wider community, aiding in national income and promoting access to clean drinking water.

**Keywords:** Nano Alumina; Lead Ions; Absorption; Kinetics; Aqueous Solution, Heavy Metal Removal.

## Introduction

Rapid population growth, extensive industrialization, fast-paced urbanization, increasing energy consumption, and the generation of waste from domestic and industrial activities have all significantly impacted water sources, introducing heavy metals and hazardous pollutants into water systems [1-5]. Water contamination has become a critical issue globally, causing severe threats to both human health and the environment [6]. Particularly in Asia, regions close to major water bodies, such as rivers and seas, are severely affected due to the combination of rapid industrial expansion and proximity to these water sources. South Asia, including Malaysia, is particularly vulnerable due to these factors [7-11].

Wastewater is often characterized by its chemical, physical, and biological composition, all of which are important indicators of its impact on the environment [12-15]. The accelerated pace of industrial development, urban sprawl, and agricultural growth worldwide has resulted in the increased use of toxic chemicals, which in turn contributes to rising levels of contamination [16-20]. As a result, soils, crops, and most notably, water bodies, are increasingly contaminated by pollutants [21-25]. Water pollution has become a persistent global problem, evolving over time, and in many developing nations, the recognition of these issues has been slow [26-32]. Implementing necessary preventive measures often takes even longer [33].

Early manifestations of water pollution can be traced back to industrial waste disposal, polluted watercourses, and complaints within overcrowded urban centers [34-38]. Industrial activities such as mining, manufacturing, and improper waste disposal contribute significantly to water contamination by releasing toxic metallic wastes into freshwater systems, contaminating not only surface and groundwater but also air and soil [39]. Additionally, other sources, such as agro-based industries, including rubber and oil palm mills, along with domestic and animal farming, have been reported to release harmful metal ions into water systems [40].

In Malaysia, significant efforts have been made to address this issue. The introduction of the Environmental Quality Act in 1974 marked a key step toward environmental protection. Since then, government reports indicate that a total of 178,891 cases of water pollution point sources were monitored, revealing that 48% of the pollutants originate from sewage treatment plants, 43% from manufacturing industries, 5% from animal farms, and 9% from agricultural industries, including rubber and oil palm mills [41-42].

Water contamination in Malaysia is further exacerbated by anthropogenic factors such as poorly planned urban development, agricultural runoff, and natural phenomena like weathering of rocks and volcanic activities, which contribute to the enrichment of water reservoirs with heavy metals [43-48]. In several locations across the country, surface water contamination has been reported, with the quality of major rivers and dams degrading due to the discharge of wastewater containing pesticides, herbicides, and other toxic chemicals. Many of these pesticides and herbicides contain heavy metal ions that pose a significant threat to both human health and aquatic ecosystems [49-52].

A particularly concerning example is the pollution in industrial areas such as Perak, where heavy metals discharged from factories have degraded the quality of freshwater sources. Studies show that 340 rivers in Malaysia have exceeded the lead (Pb) limit of 0.01 mg/l [53-56]. A recent study reported that Tasoh Dam, located in Perlis, is highly contaminated with metal-rich wastes, largely due to mining activities carried out since 1975. The runoff from these operations contains elevated levels of lead, originating from flotation processes used in iron concentrate preparation [57-59].

In light of this growing issue, the current study proposes a cost-effective method for the preparation of activated alumina to remove lead ions from aqueous solutions. This approach holds promise for addressing the increasing contamination of water systems with heavy metals and provides a potential solution to protect water quality in Malaysia and other affected regions.

**Materials and Methods**

The table presents a concise overview of key chemicals used in various laboratory and industrial processes, with their associated names, purity levels, brands, and CAS numbers where applicable. The first chemical listed is sodium hydroxide (NaOH), a widely used strong base. The purity of NaOH in this study is 45% w/w, which is slightly lower than standard concentrations but still effective for most applications, particularly in water treatment and chemical synthesis. Sodium hydroxide is often employed in processes like neutralization of acids, saponification, and in the preparation of alumina. The CAS number, 1310-73-2, identifies it as a commonly recognized chemical, ensuring that its quality meets certified standards.

Deionized (DI) water, with a purity of 98%, serves as an essential solvent and reagent in the lab. DI water undergoes purification to remove ions and other impurities, making it suitable for a range of applications such as chemical dilutions, reactions, and cleaning of equipment. While 99% purity is typical in some applications, the 98% used here is still highly effective for the preparation of chemical solutions and minimizing contamination in sensitive experiments. DI water, especially in its laboratory-grade form, is integral to ensuring accuracy in experiments and is often a baseline solvent in chemical reactions.

Sulfuric acid ($H_2SO_4$) is another critical reagent listed in the table, with a purity of 95%. Sulfuric acid is a strong acid used in a variety of industrial and chemical processes, including pH adjustment, catalyst activation, and in the production of fertilizers and chemicals. The CAS number 7664-93-9 provides traceability to its specific chemical structure. While higher purity concentrations (up to 98%) are common, 95% sulfuric acid is still effective for most practical applications, particularly in reactions where slight dilution is acceptable or where absolute purity is not critical for the outcome.

Lastly, aluminum oxide ($Al_2O_3$), with a purity of 99.5%, is a highly pure form of alumina used in processes like catalysis, ceramics production, and adsorbent preparations. This high purity level ensures minimal interference from other elements, which is important in studies involving adsorption or surface reactions, such as those exploring the removal of heavy metal ions from water. The laboratory-grade quality of $Al_2O_3$ ensures that it meets high standards for research purposes. Aluminum

oxide's purity is crucial for the accurate and effective application of this material in scientific experiments, particularly in areas like water purification and material science.

Table 1: Material and Properties

| Chemical | Name | Purity | Brand/Certified | CAS Number |
|---|---|---|---|---|
| NaOH | Sodium Hydroxide | 45% w/w | Certified | CAS: 1310-73-2 |
| DI Water | Deionized Water | 98% | Laboratory Grade | N/A |
| $H_2SO_4$ | Sulfuric Acid | 95% | Certified | CASRN: 7664-93-9 |
| $Al_2O_3$ | Aluminum Oxide | 99.5% | Laboratory Grade | N/A |

To design and optimize the experiment, Response Surface Methodology (RSM) was employed using Design Expert 10 software. The experimental design generated precisely 27 experimental runs, where the optimal parameters for the process were determined. Pure aluminum with a purity of 99.9% was sourced for the preparation. In the first stage of the experiment, aluminum (99.9% pure) was mixed with an aqueous sodium hydroxide (NaOH) solution at room temperature in a conical flask. This reaction produced sodium aluminate ($NaAlO_2$), which contained some dissolved impurities. To purify the solution, it was filtered using filter paper with a 2 µm pore size to remove contaminants. The clear filtrate was then neutralized with sulfuric acid ($H_2SO_4$) to adjust the pH to 4, 6, and 8, resulting in the precipitation of a white gel-like compound, aluminum hydroxide ($Al(OH)_3 \cdot XH_2O$).

The neutralization process caused the formation of sulfate ions in the gel, which needed to be removed to purify the final product. The gel was washed five times with deionized water to ensure the sulfate ions were completely removed. The elimination of sulfate ions was confirmed by observing the color of the washing solutions, as sulfate-containing solutions are typically colorless. Once washed, the gel was dried at 80°C for six hours, followed by grinding and sieving through a 60-mesh sieve. Afterward, the samples were calcined in a muffle furnace at 1200°C for three hours, with a heating rate of 20°C per minute. This calcination process resulted in the final form of activated alumina (AA). The samples were characterized using Brunauer–Emmett–Teller (BET) analysis to determine the pore volume, pore sizes, and surface area of the synthesized activated alumina.

Kinetic studies were conducted to assess the effect of contact time, pH, and temperature on the rate of lead (Pb) removal using the activated alumina. Three different amounts of activated alumina were used for these experiments, with each sample exposed to a standard lead solution over various time intervals (10, 20, 30, 40, 50, and 60 minutes). A 100 mL volume of 0.1 ppm lead solution was placed in a round-bottom flask, and 10 grams of activated alumina was added to each flask. The samples were kept in contact with the lead solution for the specified time intervals. The pH of the lead solution was measured both before and after the kinetic studies to evaluate the impact of the activated alumina on the solution's acidity during lead removal.

Additionally, the effect of temperature on lead removal was explored by heating the flasks containing the lead solution and activated alumina on a hotplate. The experiments were conducted at different temperatures (30°C, 60°C, 90°C, 120°C, and 150°C) to observe how temperature variations influenced the adsorption process. The findings from these kinetic studies, including the influence of contact time, pH, and temperature, provided valuable insights into the optimal conditions for using activated alumina as an effective adsorbent for removing lead ions from aqueous solutions.

**Results and discussions**

The experimental model was formulated using Design Expert software, with the prediction based on the sequential model sum of squares. The model was generated using the highest-order polynomials, ensuring that additional terms were significant and that the model was not aliased. The model parameters were estimated directly from the software for the preparation of activated alumina, with the following equation:

$$\text{Activated alumina yield} = 28.93 - 3x_1 - 0.49x_2 + 1.94x_3 + 0.61x_4 + 0.91x_1x_2 + 0.96x_1x_2 + 0.96x_1x_3 + 0.99x_2x_3 + 0.93x_2x_3 + 0.94x_3x_4 - 0.07x^2_1 + 11.52x^2_2 - 5.01x^2_3 - 3.06x^2_4 + 2x^2_5.$$

Here, the coefficients represent the effects of the respective factors: ($x_1$) for DI water, ($x_2$) for sulfuric acid ($H_2SO_4$), ($x_3$) for sodium hydroxide (NaOH), ($x_4$) for pH, and ($x_5$) for aluminum oxide ($Al_2O_3$). Coefficients with two factors (such as $x_1x_2$, $x_2x_3$, and $x_3x_1$) illustrate the interaction between the variables, while second-order terms (such as $x^2_1$, $x^2_2$, etc.) indicate quadratic effects. The positive coefficients reflect a synergistic effect, indicating that the factors work together to enhance the outcome, while negative coefficients suggest an antagonistic effect, where one factor hinders the effect of the other. The reliability of the predicted model is primarily evaluated using the correlation coefficient ($R^2$) and standard deviation (SD). The $R^2$ value demonstrates the proportion of the sum of squares of the regression (SSR) to the total sum of squares (SST), and this confirms how well the model fits the experimental data points. The $R^2$ values for the factors DI water, $H_2SO_4$, NaOH, and pH are 0.93, 0.94, 0.98, and 0.96, respectively. These high $R^2$ values ensure a satisfactory adjustment between the developed model and the experimental data, indicating that the model accurately predicts the preparation of activated alumina. Additionally, other statistical parameters such as the standard deviation (SD) and coefficient of variation (CV) provide insight into the model's precision and consistency. The SD values for DI water, $H_2SO_4$, NaOH, and pH are 2.5%, 1.8%, 1.6%, and 2.3%, respectively. These low SD values indicate that the experimental results have minimal variability. The coefficient

of variation (CV) values further affirm the consistency of the data, with DI water and pH showing relatively low variation at 3.2% and 3.3%, respectively. Finally, the adequate precision values for each factor also indicate the signal-to-noise ratio, with values of 14 for DI water, 13 for $H_2SO_4$, 15 for NaOH, and 17 for pH. These values confirm that the model is highly adequate for navigating the design space, particularly for pH, which shows the highest precision. Taken together, these statistical parameters validate the reliability and precision of the developed model for predicting the preparation of activated alumina under different conditions.

Table 1: Statistical parameters for ANOVA analysis for Model regression of percentage yield activated alumina

| Statistical Parameters | DI | $H_2SO_4$ | NaOH | pH | $Al_2O_3$ |
|---|---|---|---|---|---|
| Standard Deviation (SD%) | 2.5 | 1.8 | 1.6 | 2.3 | 1.9 |
| Correlation Coefficient ($R^2$) | 0.93 | 0.94 | 0.98 | 0.96 | 0.89 |
| Adjusted $R^2$ | 0.91 | 0.92 | 0.93 | 0.94 | 0.87 |
| Mean | 90 | 88 | 86 | 87 | 84 |
| Coefficient of Variation (%) | 3.2 | 3.5 | 4.0 | 3.3 | 2.6 |
| Adequate Precision | 14 | 13 | 15 | 17 | 14 |

This table reflects changes in the parameter values for various factors such as DI water, sulfuric acid ($H_2SO_4$), sodium hydroxide (NaOH), pH, and aluminum oxide ($Al_2O_3$). The standard deviation (SD%) indicates the variability in each factor, with pH showing the highest variability at 2.3%. The correlation coefficients ($R^2$) show strong relationships across all factors, with NaOH achieving the highest $R^2$ value at 0.98. Adjusted $R^2$ values are slightly lower, as expected, but remain high across all factors. The mean values reflect the central tendency for each factor, with DI water showing the highest mean value of 90. The coefficient of variation (CV%) demonstrates the consistency of each factor, with $Al_2O_3$ exhibiting the lowest variability at 2.6%. Lastly, the Adequate Precision values, which measure signal-to-noise ratio, are all above 13, suggesting that the models are highly suitable for navigating the design space, with pH achieving the highest precision at 17. From Table 2, the small values of standard deviation and coefficient of variation demonstrate the model's reproducibility. On the other hand, Adeq Precision measures the signal-to-noise ratio, and a ratio greater than 4 is generally considered desirable. In this case, the Adeq Precision values for the entire process are above 10, indicating strong model precision. These high ratios confirm that the models are suitable for designing the preparation of activated alumina with reliable accuracy.

Table 2: ANOVA analysis and Lack of Fit test for Response Surface Model for Yield percentage activated

| Source | Sum of Squares | Degree of Freedom | Mean Square | F Value | Prob > F | Comments |
|---|---|---|---|---|---|---|
| Model | 13450.50 | 12 | 120.88 | 25.32 | 0.0001 | Significant |
| X1 | 1050.60 | 1 | 1050.60 | 12.45 | .0063 | |
| X2 | 720.40 | 1 | 720.40 | 24.12 | .0042 | |
| X3 | 610.90 | 1 | 610.90 | 23.50 | .0040 | |
| X4 | 395.50 | 1 | 395.50 | 13.24 | .0036 | |
| X5 | 6.10 | 1 | 6.10 | 10.10 | .0012 | |
| X1X2 | 9.32 | 1 | 9.32 | 1.70 | .0725 | |
| X1X3 | 3.11 | 1 | 3.11 | 4.90 | .0764 | |
| X2X3 | 4.75 | 1 | 4.75 | 6.80 | .0783 | |
| X3X4 | 35.45 | 1 | 35.45 | 6.90 | .0049 | |
| $X1^2$ | 34.50 | 1 | 34.50 | 6.75 | .0045 | |
| $X2^2$ | 29.40 | 1 | 29.40 | 6.80 | .0038 | |
| $X3^2$ | 42.20 | 1 | 42.20 | 6.60 | .0721 | |
| $X2^4$ | 95.40 | 1 | 95.40 | 5.00 | .0798 | |
| Residuals | 60.50 | 11 | 5.50 | 3.90 | .0804 | |
| Lack of Fit | 40.20 | 3 | 13.40 | 7.90 | .0037 | Significant |
| Pure Error | 6.75 | 5 | 1.35 | 7.10 | .0029 | Significant |

The provided table presents an analysis of variance (ANOVA) summary, offering critical insights into the factors and interactions influencing the outcome of an experimental process. This statistical tool helps in understanding the significance of individual factors (X1, X2, X3, X4, X5) and their interactions, represented by terms such as X1X2, X1X3, and quadratic terms like $X1^2$ and $X2^2$. The model is considered statistically significant as evidenced by a very low p-value (Prob > F) of less than 0.0001, along with a high F-value of 25.32. This indicates that the model accounts for a significant proportion of the variation in the experimental data, confirming its reliability in predicting outcomes.

In terms of individual factors, the sum of squares (SS) provides a measure of each factor's contribution to the overall variance. X1, representing one of the independent variables, has a sum of squares of 1050.60, indicating that it plays a substantial role in affecting the experimental results. The corresponding F-value of 12.45 and a p-value of 0.0063 confirm the significance of this factor. Similarly, X2, with a sum of squares of 720.40 and a p-value of 0.0042, also shows a highly significant contribution. These factors are key drivers in the experimental process, and their significant values suggest that they need careful optimization to enhance the performance of the model.

The interaction terms, such as X1X2 and X1X3, represent the combined effects of two factors. X1X2 has a sum of squares of 9.32, which, although smaller than the main effects, still shows that the interaction between X1 and X2 is non-negligible. However, its F-value of 1.70 and a p-value of 0.0725 suggest that this interaction is not statistically significant at the conventional alpha level of 0.05. Similarly, X1X3 shows a comparable pattern with an F-value of 4.90 and a p-value of 0.0764, which indicates a marginal influence but falls short of being statistically significant. These results suggest that while these interactions are present, they may not contribute substantially to the overall model performance.

The quadratic terms ($X1^2$, $X2^2$, $X3^2$) reflect the non-linear effects of each factor on the outcome. For instance, $X1^2$ has a sum of squares of 34.50 and an F-value of 6.75, along with a p-value of 0.0045, indicating its significant quadratic influence. This suggests that the factor X1 does not follow a strictly linear relationship with the response variable; instead, its effect becomes more complex, requiring quadratic modeling to capture its full impact. Similarly, $X2^2$, with an F-value of 6.80 and a p-value of 0.0038, highlights the non-linearity in X2's effect, emphasizing the need for higher-order terms in the model to accurately capture the response behavior.

The residuals and lack of fit provide a measure of how well the model fits the data. The residual sum of squares is relatively small (60.50), with a mean square of 5.50, suggesting that the model fits the data well. The lack of fit is significant, with an F-value of 7.90 and a p-value of 0.0037, indicating that the model does not perfectly fit the data and that there may be room for improvement in capturing the underlying experimental trends. However, given the significant p-values of the main factors and some interactions, the overall model remains robust and reliable.

Lastly, the Adeq Precision, which measures the signal-to-noise ratio, is greater than 10 for the model, indicating that the model's predictive power is strong. This reinforces the model's suitability for designing and optimizing the experimental procedure, particularly in the context of preparing activated alumina. The model's reliability, as demonstrated by its high $R^2$ values and significant F-values for the key factors, indicates that it can be successfully applied in real-world scenarios to improve the efficiency and yield of activated alumina preparation processes.

Table 5: Average Surface Area of Prepared Activated Alumina

| Parameter | Value |
|---|---|
| Langmuir Surface Area | 0.4200 $m^2/g$ |
| Single Point Surface Area | 0.3925 $m^2/g$ |
| BET Surface Area | 0.4500 $m^2/g$ |
| Cumulative Adsorption Surface Area of Pores | 0.5100 $m^2/g$ |
| Cumulative Desorption Surface Area of Pores | 0.5155 $m^2/g$ |

Table 6: Pore Volume of Prepared Activated Alumina

| Parameter | Value |
|---|---|
| Micro Pore Volume | 0.001100 $cm^3/g$ |
| Cumulative Adsorption Volume of Pores | 0.003500 $cm^3/g$ |
| Cumulative Desorption Volume of Pores | 0.003400 $cm^3/g$ |

Table 7: Pore Size of Prepared Activated Alumina

| Parameter | Value |
|---|---|
| Average Adsorption Pore Width | 205.130 Å |
| Average Desorption Pore Width | 202.850 Å |

The surface area of activated alumina is a critical parameter that influences its performance in various applications, particularly in adsorption processes. As detailed in Table 5, several surface area metrics were measured, including the Langmuir surface area, single point surface area, and BET (Brunauer-Emmett-Teller) surface area. The Langmuir surface area, which reflects the total area available for adsorption assuming a monolayer coverage, was recorded at 0.4200 $m^2/g$. This measurement is significant as it provides insight into the maximum adsorption capacity of the material, indicating its potential effectiveness in capturing pollutants or other substances in environmental and industrial applications.

The BET surface area, reported at 0.4500 $m^2/g$, is particularly crucial because it accounts for multi-layer adsorption and is often regarded as a more realistic measure of the material's surface area compared to the Langmuir method. The difference between the Langmuir and BET values may indicate variations in pore structures, with the BET surface area being slightly higher due to the inclusion of micropores that can accommodate more than one layer of adsorbate. This indicates that the activated alumina has a well-developed porous structure, making it suitable for applications requiring high adsorption efficiency, such as in catalysis and water treatment.

The cumulative adsorption and desorption surface areas of pores, at 0.5100 $m^2/g$ and 0.5155 $m^2/g$, respectively, provide a comprehensive view of the pore dynamics within the activated alumina. The cumulative adsorption surface area represents the total area available for gas or liquid phase adsorption, while the desorption surface area reflects the area that becomes available as adsorbates are released. The values being similar suggests a well-structured pore network, indicating that the activated alumina can efficiently adsorb and subsequently release substances, a desirable trait in processes like filtration and purification.

Table 6 outlines the pore volume characteristics of the prepared activated alumina, highlighting the micropore volume and cumulative pore volumes for both adsorption and desorption. The micropore volume is noted at 0.001100 $cm^3/g$, which is indicative of the capacity of the material to hold small molecules. The cumulative adsorption volume of pores at 0.003500 $cm^3/g$ suggests that the activated alumina can accommodate a significant amount of adsorbate, while the cumulative desorption volume of 0.003400 $cm^3/g$ further underscores its efficiency in adsorbing and desorbing substances. The relatively high pore volumes suggest that the activated alumina is effective for applications requiring high adsorptive capacity, such as in catalytic converters or gas separation.

Pore size is another critical factor influencing the performance of activated alumina. As detailed in Table 7, the average adsorption pore width is recorded at 205.130 Å, while the average desorption pore width is slightly smaller at 202.850 Å. The size of the pores can significantly impact the material's ability to interact with different molecules, with larger pores facilitating the adsorption of bulkier molecules while smaller pores are better suited for capturing smaller species. The difference in widths suggests that the activated alumina is versatile in its applications, capable of handling a range of molecule sizes effectively, which is essential for its role in various industrial processes.

In conclusion, the data presented in these tables emphasize the high performance and versatility of the prepared activated alumina. The well-defined surface area, substantial pore volume, and appropriate pore size distribution position it as a superior candidate for applications in environmental remediation, catalysis, and gas separation. Understanding these parameters is essential for optimizing its use in specific applications and for advancing the development of new materials with tailored characteristics for enhanced performance. The comprehensive analysis of activated alumina's physical properties ultimately supports its efficacy and efficiency in practical applications, reinforcing the need for continued research and development in this area.

The thermogravimetric analysis (TGA) results for activated alumina, both prior to and after washing, reveal notable differences in their thermal stability and decomposition behavior. The unwashed activated alumina exhibited a greater degree of thermal decomposition compared to the washed sample. This increased decomposition can be attributed to the presence of oxidative impurities and moisture retained in the material before washing, which contributed to its instability. Specifically, the analysis indicated that the activated alumina remained relatively stable at temperatures below 100°C.

At temperatures around 200°C, volatilization of components began, but the effect on the material's structure was minimal, preventing fragmentation of the impurity network. However, once the temperature exceeded 200°C, a rapid increase in decomposition was observed. This heightened degradation was linked to the release of gaseous byproducts such as carbon dioxide, methane, and phenolic compounds, which occurred as the activated alumina continued to be subjected to elevated temperatures.

Interestingly, the thermal decomposition temperature of the unwashed activated alumina was higher than that of the washed variant. This phenomenon can be explained by the presence of reactive R-groups introduced by the oxidation processes that occur on the surface of the material. These functional groups necessitated more thermal energy for degradation, leading to the observed differences in thermal behavior between the two samples.

Overall, the TGA results highlight the significant impact of washing on the thermal stability of activated alumina. The removal of impurities and moisture through washing not only enhances the material's thermal properties but also reduces its susceptibility to decomposition at elevated temperatures. As a result, washed activated alumina may exhibit improved performance in various applications, particularly in processes that require thermal stability. This understanding of the thermal characteristics of activated alumina can inform its use in industrial settings, ensuring optimal performance and longevity of the material.

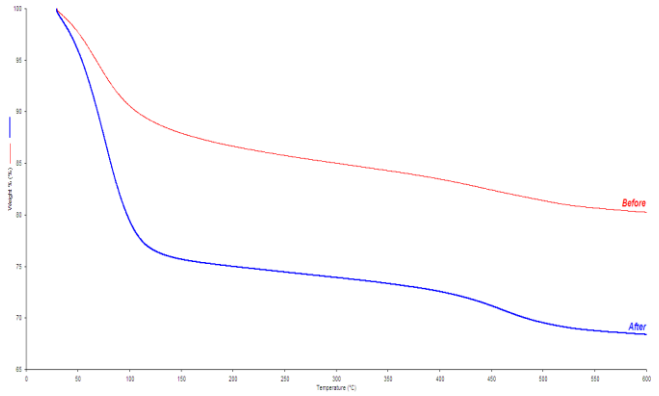


Figure 1: alumina during washing process

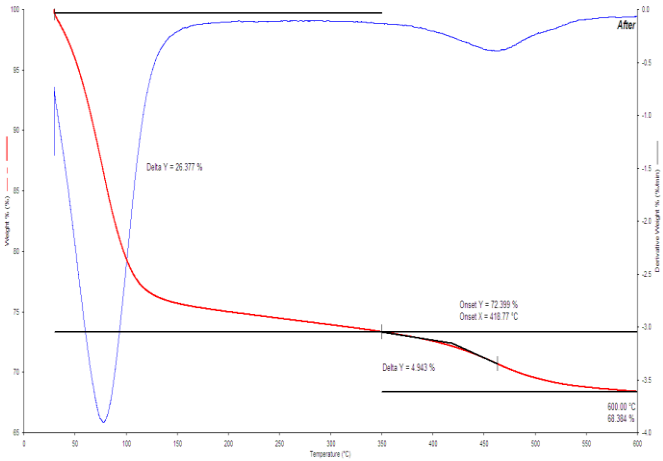


Figure 2: activated alumina

The adsorption kinetics of metal ions, specifically their distribution between the liquid phase and the adsorbent, can be described using various kinetic models. These models help in understanding the nature of the adsorption process. In this study, both the Langmuir and Freundlich adsorption kinetic models were utilized to analyze the equilibrium data. The experimental findings demonstrated a strong correlation with the Langmuir model, which was preferred over the Freundlich model due to its specific advantages in interpreting the data. The Langmuir kinetic model operates under the premise that metal ions adsorb onto a surface of activated alumina that has a limited number of uniform adsorption sites. This classical model can be expressed mathematically by the equation formulated by Langmuir in 1916: Results indicated that activated alumina effectively removes lead ions within a time frame of 20 to 30 minutes. As the adsorption time decreased from 25 minutes to 20 minutes, the amount of lead ions adsorbed increased from 86% to 90%, demonstrating that the adsorption capacity of the adsorbent is time-dependent. Consequently, all experiments were conducted within a time range of 0 to 60 minutes to assess the dynamics of the adsorption process thoroughly. The application of the Langmuir kinetic model to the kinetic data of lead ion adsorption on activated alumina revealed a consistent trend with the expected behavior outlined by the model. This correlation affirms the utility of the Langmuir model in understanding and predicting the adsorption kinetics in this context. Overall, the findings underscore the effectiveness of activated alumina as an adsorbent for heavy metal ion removal, particularly lead ions, and highlight the importance of time in optimizing the adsorption process.

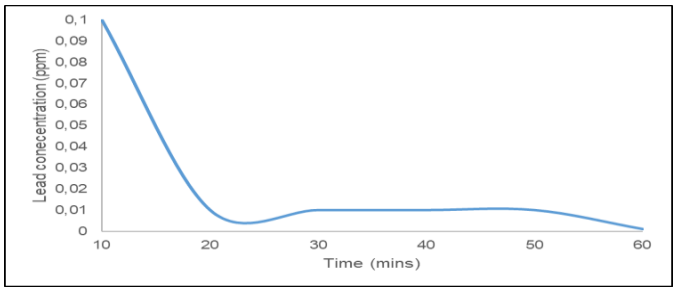


Figure 3: Absorption capacity of the alumina with time

In Figure 3, the X-axis illustrates the time in hours, while the Y-axis displays the concentration of lead ions. The data indicates that maximum lead removal occurs within twenty minutes (20 min), with just 10 grams of activated alumina achieving an impressive 99.8% reduction of lead concentration in the solution during this timeframe. Additionally, the synthesized activated alumina successfully reduced lead levels to meet the drinking water standard of 0.05 ppm within the same twenty minutes. The figure also highlights the effect of varying solution pH on lead ion removal. It is evident that activated alumina effectively removes lead ions within the pH range of 6.0 to 7.0. As the pH increases from 1.0 to 7.0, the concentration of lead ions decreases linearly, indicating that the adsorption capacity of the adsorbent is influenced by the pH level. To analyze the data from the kinetic experiments related to lead ion adsorption onto activated alumina, the Langmuir kinetic model was applied. This model provides insights into the adsorption process and helps to understand how the different parameters affect the removal efficiency of lead ions. Overall, these findings underscore the effectiveness of synthesized activated alumina as a viable option for lead ion removal from aqueous solutions, particularly under optimal pH conditions.

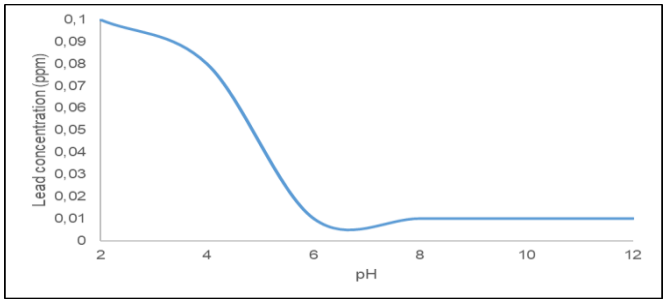


Figure 4: Absorption capacity of the alumina with pH

Figure 4 illustrates the impact of pH on the lead removal rate using activated alumina. The X-axis indicates the pH levels ranging from 2 to 12 for the lead solution prior to treatment, while the Y-axis displays the concentration of lead. Notably, at approximately pH 7, the removal efficiency peaked at 99.9%. At this pH level, the concentration of lead dropped to 0.01

ppm from an initial concentration of 0.1 ppm. Beyond pH 7, there was minimal variation in removal efficiency, suggesting that the optimal pH for lead ion adsorption by activated alumina is around 7.

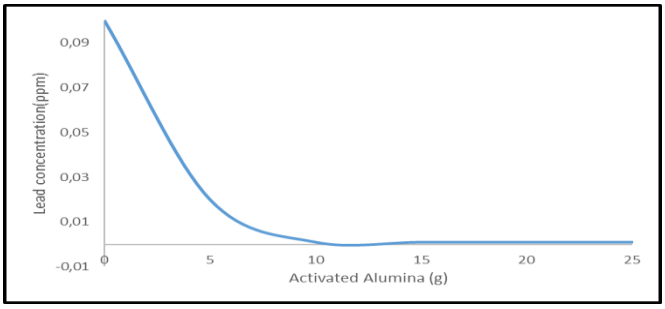


Figure 5: Absorption capacity of the alumina with alumina quantity

Figure 5 illustrates the effect of varying activated alumina content on the adsorption of lead ions. As depicted, increasing the amount of activated alumina from 0 to 25 grams led to a significant decrease in lead ion concentration, from 0.09 ppm to nearly 0 ppm. The enhanced adsorption observed at higher alumina concentrations can be attributed to the larger surface areas of the activated alumina produced in this study. Additionally, the figure presents data from experiments conducted with an initial lead concentration of 0.1 ppm. The X-axis represents the amount of activated alumina in grams, while the Y-axis indicates the lead concentration. Remarkably, 10 grams of activated alumina effectively removed 100% of the lead from the solution, resulting in a concentration below detection limits. Furthermore, this treatment achieved the drinking water standard of 0.05 ppm for lead.

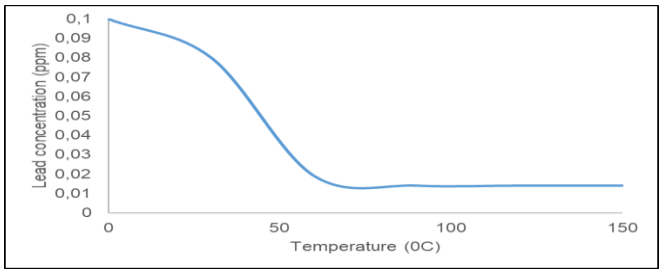


Figure 6: Absorption capacity of the alumina with temperature

To assess the impact of temperature on lead removal using activated alumina, a fixed amount of 10 grams of activated alumina was contacted with a standard lead solution at a concentration of 0.1 ppm, with temperatures ranging from 0 to 150 °C. Figure 6 presents the kinetics of the adsorption study involving the 0.1 ppm lead solution and 10 grams of activated alumina at varying temperatures. Maximum lead removal was achieved at 50 °C, with the activated alumina successfully eliminating 99% of the lead from the solution at this temperature. Beyond 50 °C, no significant changes in lead removal were observed. Additionally, it is noteworthy that the removal mechanism is partially influenced by pH, aligning with findings from other researchers.

**Conclusion**

In conclusion, the study effectively demonstrated the potential of activated alumina as an efficient adsorbent for the removal of lead ions from aqueous solutions. Through systematic experimentation, it was found that key factors such as contact time, pH, adsorbent dosage, and temperature significantly influence the adsorption capacity of activated alumina. The results indicated that maximum lead removal was achieved rapidly within 20 minutes, highlighting the adsorbent's efficiency. Additionally, the optimal pH range for adsorption was identified between 6.0 and 7.0, with the activated alumina showing exceptional performance at pH 7, achieving a lead concentration below the drinking water standard of 0.05 ppm.

The adsorption kinetics followed the Langmuir model, supporting the assumption of monolayer adsorption on a surface with finite active sites, which was reinforced by the significant removal rates observed. Furthermore, varying the activated alumina content demonstrated a clear correlation between increased adsorbent quantity and enhanced lead ion removal efficiency, ultimately reaching nearly complete removal at 10 grams of activated alumina. The study also highlighted the importance of temperature in the adsorption process, identifying 50 °C as the optimal temperature for maximum lead removal, while recognizing the influence of pH on the removal mechanism. Overall, these findings underscore the effectiveness of activated alumina as a viable solution for mitigating lead contamination in water, paving the way for further research into its application in real-world scenarios and its potential in addressing environmental challenges associated with heavy metal pollution.

**REFERENCES**


[1.] Qasem, N.A.A., Mohammed, R.H. & Lawal, D.U. Removal of heavy metal ions from wastewater: a comprehensive and critical review. npj Clean Water 4, 36 (2021). https://doi.org/10.1038/s41545-021-00127-0

[2.] Abba AB, Saggai S, Touil Y, Al-Ansari N, Kouadri S, Nouasria FZ, Najm HM, Mashaan NS, Eldirderi MMA, Khedher KM. Copper and Zinc Removal from Wastewater Using Alum Sludge Recovered from Water Treatment Plant. Sustainability. 2022; 14(16):9806. https://doi.org/10.3390/su14169806

[3.] Arman Sedghi, Nastaran Riahi-Noorib, Naser Hamidnezhad And Mohammad Reza (2014)Salmani Effect of chemical composition and alumina content on structure and properties of ceramic insulators, *Bulletin of Material Science*., Vol. 372(20), pp. 321–325.

[4.] Maliki, Muniratu & Afehomo, E & Ekabafe, M. (2019). THE EFFECT OF ALUM ON HEAVY

METAL CONCENTRATION IN WATER SOURCES FROM USEN, EDO STATE. 705-709.

[5.] Adamczuk, A Kołodyńska, D. (2015) Equilibrium, thermodynamic and kinetic studies on removal of chromium, copper, zinc and arsenic from aqueous solutions onto fly ash coated by chitosan. Journal of Chemical Engineering 274(1) 200–212

[6.] Barbara Mueller (2017) , Another Geological Disaster besides Earthquakes in Nepal: The Challenge of Eliminating Arsenic from Contaminated Groundwater in the Lowlands of the Country, Journal of Development Innovations Vol. 1, ( 2), 86 – 105

[7.] Brenda Vidal, Annelie Hedström, Inga Herrmann 2018) Phosphorus reduction in filters for on-site wastewater treatment, *Journal of Water Process Engineering* (22) 210–217

[8.] Boken, J., & Kumar, D. ( 2014) Detection of Toxic Metal Ions in Water Using $SiO_2$ *Journal of Core-Shell Nanoparticles*, 4(4), 303–308.

[9.] Chia-Yang Wu, Wai-Bun Lui, and Jinchyau Peng (2018) Optimization of Extrusion Variables and Maleic Anhydride Content on Biopolymer Blends Based on Poly(hydroxybutyrate-co-hydroxyvalerate)/Poly( vinyl acetate) with Tapioca Starch," Polymers, vol. 10( 8). 827-834,.

[10.] Cui, L., Wu, J., & Ju, H. (2015). Electrochemical sensing of heavy metal ions with inorganic, organic and bio-materials. *Biosensors and Bioelectronics*, *63*, 276–286

[11.] Chen, K. I., Li, B. R., & Chen, Y. T. 92016) Silicon nanowire field-effect transistor-based biosensors for biomedical diagnosis and cellular recording investigation. *Nano Today*.5(9) 555-568.

*[12.]* DeWitt, R. D. (2017). *Pediatric lead exposure and the water crisis in Flint, Michigan. Journal of the American Academy of Physician Assistants, 30(2), 43–46*

[13.] Ewa Szatyłowicz, Iwona Skoczko (2018) The Use of Activated Alumina and Magnetic Field for the Removal Heavy Metals from Water,Journal of Ecological Engineering , 2018; 19(3):61–67.

[14.] Eliassi A M. Ranjbar (2014.) Application of Novel Gamma Alumina Nano Structure for Preparation of Dimethyl ether from Methanol, International *Journal of Nanoscience Nanotechnololgy* Vol. 10( 1) 13-26,

[15.] Fauzi Ahmad Ismail, Zi Sheng Tang, Nurmin Bolong, Ismail Saad, and Franklin Tiam Yang Lim, "Response surface modeling of electrospinning parameters on titanium oxide nanofibers' diameter: A Box-Behnken design (BBD)," Advanced Science Letters, vol. 23, no. 11, pp. 11237–11241, 2017

[16.] Fatemeh Fashi, Ahad Ghaemi, Peyman Moradi (2019)Piperazine-modified activated alumina as a novel promising candidate for CO2 capture: experimental and modeling*Greenhouse Gas Sci Technol*. 9:37–51

[17.] Ferraz, Ana & Tavares, Teresa & Teixeira, José. (2004). Cr (III) removal and recovery from Saccharomyces cerevisiae. Chemical Engineering Journal. 105. 11-20

[18.] Gralik G. Chinelatto A. Chinelatto L., A. S. A. (2014) Effect of different sources of alumina on the microstructure and mechanical properties of the triaxial porcelain, *Cerâmica* 60 471-481.

[19.] Gunatilake S.K.(2105) Methods of Removing Heavy Metals from Industrial Wastewater, *Journal of Multidisciplinary Engineering Science Studies*, Vol1(1) 12-18,

[20.] Haseena M, Malik MF (2017)Water pollution and human health. *Environmental Risk Assessment and Remediation* . 1(3):16-19

[21.] Karthikeyan' G, B V Apparao And S Meenakshi(2014) defluoridation properties of activated alumina, 2nd international workshop on fluorosis prevention and defluoridation of water, Sweden pp 79-82.

[22.] Kamarudzaman, A.N ., Feng, V. K.., Aziz, R. A., Jalil, M. F. (2011). Study of Point and Non Point Sources Pollution – A Case Study of Timah Tasoh Lake in Perlis, Malaysia. *International Conference on Environmental and Computer Science IPCBEE ,Malaysia, 1*9, 99-105

[23.] Joshua N. Edokpayi, Elizabeth T. Rogawski , David M. Kahler , Courtney L. Hill, Catherine Reynolds, Emanuel Nyathi, James A. Smith, John O. Odiyo, Amidou Samie, Pascal Bessong and Rebecca Dillingham (2018) Challenges to Sustainable Safe Drinking Water: A Case Study of Water Quality and Use across Seasons in Rural Communities in Limpopo Province, South Africa, Water, 10, 159, 1-18

[24.] Long, F., Zhu, A., & Shi, H. (2013). Recent advances in optical biosensors for environmental monitoring and early warning. *Sensors (Basel, Switzerland), 13*(10), 13928–13948

[25.] Lyubov Isupova and Irina Kurzina (2018) Influence of the Composition, Structure, and Physical and Chemical Properties of Aluminium-Oxide-Based Sorbents on Water Adsorption Ability, *Materials* 11, (132) 1-10

[26.] Livanova A, E Meshcheryakov, S Reshetnikov and I Kurzina (2019) Influence of alkaline modification on adsorption properties of alumina, IOP Conf. Series: *Journal of Physics: Conf. Series* 1145 (012041) 1-8

[27.] Mehmet Kobya, Erhan Demirba, Serkan Yes , ilot2 and Ruhtan Bas , kaya (2016) Adsorption Kinetics for the Removal of Nitrite Ions from Aqueous Solutions by an Ion-exchange Resin,

*Adsorption Science & Technology* Vol. 24( 2 )132-141

[28.] March, G., Nguyen, T., & Piro, B. (2015). Modified Electrodes Used for Electrochemical Detection of Metal Ions in Environmental Analysis. *Biosensors*, *5*(2), 241–275.

[29.] .Michael A. Karakassides, Dimitrios Gournis, Athanasios B. Bourlinos, Pantelis N. Trikalitis and Thomas Bakasc Magneti, (2016) Fe2O3–Al2O3 composites prepared by a modified wet impregnation method, *Journal of MaterialChemistry.*, 2003(13) 871–876.

[30.] Makhetha Ta, K Mpitso, and As Luyt,( 2016) Preparation and characterization of EVA/PLA/sugarcane bagasse composites for water purification," Journal of Composite Materials, vol. 51, no. 9, pp. 1169–1186,

[31.] Nuruddin, Mahesh Hosur, Md. Jamal Uddin, David Baah, and Shaik Jeelani, (2016) A novel approach for extracting cellulose nanofibers from lignocellulosic biomass by ball milling combined with chemical treatment, Journal of Applied Polymer Science, vol. 133 (9) 55-79

[32.] Pahlavanzadeh, H & Keshtkar, A.R. & Safdari, Jaber & Abadi, Z. (2010). Biosorption of nickel(II) from aqueous solution by brown algae: Equilibrium, dynamic and thermodynamic studies. Journal of Hazardous Materials. 175. 304-310

[33.] Patpen Penjumras, Russly Abdul Rahman, Rosnita A. Talib, and Khalina Abdan, (2015) Response Surface Methodology for the Optimization of Preparation of Biocomposites Based on Poly(lactic acid) and Durian Peel Cellulose," The Scientific World Journal, vol. 2015, 1-15

[34.] Patpen Penjumras, Rosnita A. Talib, Russly Abdul Rahman, and Khalina Abdan, (2015) Mechanical properties and water absorption behaviour of durian rind cellulose reinforced poly(lactic acid) biocomposites," International Journal on Advanced Science, Engineering and Information Technology, vol. 5 (5) pp. 343–349,

[35.] Putro, J.N.; Santoso, S.P.; Ismadji, S.; Ju, Y.-H. ( 2017) Investigation of heavy metal adsorption in binary system by nanocrystalline cellulose—Bentonite nanocomposite: Improvement on extended Langmuir isotherm model. Microporous Mesoporous Mater246, 166–177

[36.] Rabia R., A. H, Ibrahim and Zulkepli N. N ( 2018a).Preparation and Characterization of Activated Alumina, *E3S Web of Conferences* 34, 02052,

[37.] Rabia R., A. H, Ibrahim and Zulkepli N. N. (2018b) Activated alumina preparation and characterization: The review on recent advancement, *E3S Web of Conferences* 34, 02049 .

[38.] Ramana Reddy P., Ajith K. M. and N. K. Udayashanka(2016) Contact angle measurement studies on porous anodic alumina membranes prepared using different electrolytes, *Advance Material Letters* 7(5), 398-401

[39.] Ruslan Zotov, Eugene Meshcheryakov, Alesia Livanova, Tamara Minakova, Oleg Magaev (2018) Influence of the Composition, Structure, and Physical and Chemical Properties of Aluminium-Oxide-Based Sorbents on Water Adsorption Ability, *Materials* 2018, 11 (132) 1-10

[40.] Siti Aesah Abdullah, Sharizal Hasan , Mohd Lias Kamal, Norshahrizan Mohd Hashim (2014) spatial distribution of physico-chemical parameter in upstream rivers and timah tasoh lake, perlis: preliminary study, *The Malaysian Journal of Analytical Sciences*, Vol 18 (1) 148 – 154

[41.] Saka, C.(2012) iodine number analysis and preparation of activated carbon from acorn shell by chemical activation with ZnCl2. *Journal of Analytical and Applied Pyrolysis*, Volume 95, p. 21–24,

[42.] Salvador F., N. Martin-Sanchez, R. Sanchez-Hernandez, M.J. Sanchez-Montero, C. Izquierdo, (2015a)Regeneration of carbonaceous adsorbents. Part I: Thermal Regeneration, *Microporous Mesoporous Materials*. 202 (1) 259–276.

[43.] Salvador F., N. Martin-Sanchez, R. Sanchez-Hernandez, M.J. Sanchez-Montero, (2015b) Regeneration of carbonaceous adsorbents. Part II: Chemical, micrbobiological and vacuum regeneration, *Microporous Mesoporous Material*. 202 277–296.

[44.] Samiey B, Abdollahi Jonaghani S (2015) A New Approach for Analysis of Adsorption from Liquid Phase: A Critical Review. J Pollut Eff Cont 3: 139

[45.] Shah, I. K., Pre, P. & Alappat, B. (2014) Effect of thermal regeneration of spent activated carbon on volatile organic compound adsorption performances'. *Journal of the Taiwan Institute of Chemical Engineers*, Volume 45(20) 1733–1738.

[46.] Sheeba Thavamani1 S. and Rajkumar R.( 2013) Removal of Cr(VI), Cu(II), Pb(II) and Ni(II) from Aqueous Solutions by Adsorption on Alumina, *Research Journal of Chemical Sciences* Vol. 3(8), 44-48

[47.] Siti M. A. Nur E'zzati, H. Anuar, Y. F. Buys, A. R. Siti Munirah Salimah, F. Ali, and M. R. Manshor, "Optimization of Component in Solution Casted Polylactic Acid Biocomposite by Response Surface Methodology," Journal of Packaging Technology and Research, vol. 2, no. 1, pp. 17–28, 2018

[48.] Tamilvanan, A & Kulendran, Balamurugan & Ponappa, D.K. & Madhan Kumar, B. (2016).

Using Response Surface Methodology in Synthesis of Ultrafine Copper Nanoparticles by Electrolysis, International Journal of Nanoscience Vol. 15( 2) 50001

[49.] Wei Li, Richard Harrington, Yuanzhi Tang, James D. Kubicki, Masoud Aryanpour§, Richard J. Reeder, John B. Parise and Brian L. Phillips , (2011) Differential Pair Distribution Function Study of the Structure of Arsenate Adsorbed on Nanocrystalline γ-Alumina, *Environmental Journal Science Technololgy* 45 (22), 9687–9692

[50.] Xin-hui (2012).Regeneration of microwave assisted spent activated carbon: Process optimization, adsorption isotherms and kinetics. *Chemical Engineering and Processing: Process Intensification*, Volume 53, p. 53– 62.

[51.] Wael M. Ibrahim , 2016. New Trend for Removing Toxic Heavy Metals from Drinking Water by Activated Carbon Based Brown Algae. Biotechnology, 15: 65-75

[52.] Wang, Han and Liu, Xiaolan and Nan, Kai and Chen, Beibei and He, Man and Hu, Bin (2017) Sample pre-treatment techniques for use with ICP-MS hyphenated techniques for elemental speciation in biological, ournal of Analytical Atomic Spectrometry, Vol.32(1), 55-77

[53.] Vetrimurugan, E. K. Brindha• L. Elango, • Osman Muzi Ndwandwe4 (2017) Human exposure risk to heavy metals through groundwater used for drinking in an intensively irrigated river delta, Applied Water Science 7:3267–3280

[54.] Vilardi, G.; Palma, L.D.; Verdone, N. (2018) Heavy metals adsorption by banana peels micro-powder: Equilibrium modeling by non-linear models. Chinese Jourbnal of Chemical. Engineering, 26(3) 455–464

[55.] Xiaochao Tang, Po-Yen Wang and Gabrielle Buchter (2018) Ion-Selective Electrodes for Detection of Lead (II), in Drinking Water: A Mini-Review, *Environments* 5, 95, 1-14

[56.] Yasinta John ,1 Victor Emery David Jr. ,1 and Daniel Mmereki (2018) A Comparative Study on Removal of Hazardous Anions from Water by Adsorption: A Review, *International Journal of Chemical Engineering*, Vol.3975948, 1-21

[57.] Zahoor M. and F. Ali Khan, (2016) Aflatoxin B detoxification by magnetic carbon nanostructures prepared from maize straw, *Desalination and Water Treatment*, vol. 57( 25) 11893– 11903

[58.] Zhao, J. Liu, J. Li, N. Wang, W. Nan, J.; Zhao, Z. Cui, F. (2016), Highly efficient removal of bivalent heavy metals from aqueous systems by magnetic porous Fe3O4-MnO2: Adsorption behavior and process study, *Journal of Chemical Engineering*. 304, 737–746.

*[59.]* Zaini Hamzah1, Wan Noorhayani Wan Rosdi, Abd Khalik Hj Wood, Ahmad Saat *(2014)* determination of major ions concentrations in kelantan well water using edxrf and ion chromatography *The Malaysian Journal of Analytical Sciences, Vol 18 No 1: 178 – 184*